Available online at www.sciencedirect.com

ScienceDirect

Procedia CIRP 144 (2026) 240–245

www.elsevier.com/locate/procedia

8th CIRP Conference on Surface Integrity

Introduction of compressive residual stresses by Hammering Turning

Jannik Schwalm*, Volker Schulze, Frederik Zanger

wbk Institute of Production Science, Karlsruhe Institute of Technology (KIT), Kaiserstr. 12, 76131 Karlsruhe, Germany

* Corresponding author. Tel.: +49-721-608-42455; fax: +49-721-608-45005. E-mail address: jannik.schwalm@kit.edu

Abstract

The process combination of Hammering Turning is an advanced development of vibration-assisted machining (VAM), which integrates a combination of microtexturing of the surface and mechanical surface treatment into the machining process. This investigation compared the process combination of Hammering Turning with conventional turning and single-axis vibration-assisted machining. In the Hammering Turning process, a two-axis vibration is superimposed on the cutting tool in an external longitudinal turning process, which is synchronized in both axes and with the cutting speed. This hammer-like movement of the cutting tool induces a deep plastic deformation of the surface layer, which in turn causes the introduction of compressive residual stresses.

This work investigates the influence of the process parameters feed rate, frequency, and amplitude of the Hammering Turning on the compressive residual stresses in the surface layer. The compressive stresses introduced by Hammering Turning are compared and correlated with those of a conventional turning process and a modified single-axis vibration-assisted machining.

The results show that Hammering Turning can achieve comparable compressive residual stresses of $\sigma < -1100$ MPa for conventional mechanical surface treatment when machining AISI 4140 quenched and tempered steel.

© 2026 The Authors. Published by Elsevier B.V.
This is an open access article under the CC BY-NC-ND license (https://creativecommons.org/licenses/by-nc-nd/4.0)
Peer-review under responsibility of the scientific committee of the Scientific committee of the CIRP CSI 2026

Keywords: Residual stresses; vibration-assisted machining; mechanical surface treatment

1. Introduction

In vibration-assisted machining (VAM), at least one additional motion component with a small amplitude and high frequency is superimposed to the cutting movement of the tool [1]. The first scientific implementation of vibration-assisted turning took place in 1968 with the use of an electrohydraulic servo system. This system operated at frequencies between 0 Hz and 125 Hz with an amplitude of 0.1 mm [2]. It resulted in a significant reduction in feed force, whereas the reduction in tangential force was minimal. However, vibration-assisted machining not only improves the chip formation itself, but also offers the possibility of influencing the surface integrity in a targeted manner. By exciting the tool with a vibration, microtextures can be created on component surfaces. Greco et al. introduced the term “vibromechanical texturing” (VMT) for this process [3]. In addition to the topography, this advanced machining process offers the possibility of inducing residual stresses during machining. In vibration-assisted machining, varying residual stresses in cutting direction can occur due to locally varying cutting speeds and cutting depths. The calculation of a periodic distribution of residual stresses was achieved through the utilization of a two-dimensional mathematical model. This calculation method was developed by Huang & Zhang et al. for the analytical, closed-form calculation of residual stresses.[4]. This depends on the phase shift of the tool paths and the resulting variation in chip thickness. A numerical and analytical investigation of two-dimensional vibration-assisted machining of Ti6Al4V was carried out by Kurniawan & Ahmed. It was found that high compressive residual stresses can occur, which are due to a hammer-like effect of the tool and an increased cutting speed [5]. In the investigation of vibration-assisted turning of the same material by Maroju & Pasam, the analysis was carried out experimentally and by simulation. An ultrasonic system with an amplitude of 20 µm and a frequency of 20 kHz was used. The

2212-8271 © 2026 The Authors. Published by Elsevier B.V.
This is an open access article under the CC BY-NC-ND license (https://creativecommons.org/licenses/by-nc-nd/4.0)
Peer-review under responsibility of the scientific committee of the Scientific committee of the CIRP CSI 2026
10.1016/j.procir.2026.02.072

experiments and simulations showed a 35% increase in compressive residual stresses, whereas tensile stresses were present in conventional machining [6]. This observation is attributed to the lower temperature during vibration-assisted machining. The process of Hammering Turning is a process combination that integrates mechanical surface treatment with vibration-assisted machining. The process uses two piezoelectric actuators operating in the non-resonant frequency range to enable simultaneous machining, mechanical surface treatment, and microtexturing. Due to their orthogonal arrangement, the actuators provide synchronized kinematics that decouple the vertical hammer movement from the tangential cutting process. One actuator performs a sinusoidal tool movement in the cutting direction, which results in a superposition with the cutting speed, periodically leading to a relative tool-workpiece speed close to zero during hammering. A detailed mathematical derivation of Hammering Turning can be found in [7]. This study investigates the residual stresses achieved during Hammering Turning. These are compared with those achieved by single-axis vibration-assisted turning and conventional turning.

2. Experimental setup

2.1. Process parameters

The investigations focus on analyzing the effects of the process combination of Hammering Turning with decoupled cutting and hammering movements on the residual stresses in the surface layer. Three variants were considered: The Hammering Turning process, a variant of single-axis vibration-assisted cutting without decoupling the sliding speed – in the following referred to as vibration-assisted turning – and a conventional turning process with identical parameters as a reference. All tests were carried out as external longitudinal turning processes with the process parameters specified in Table 1. For each set of parameters, one test was performed. The tool kinematics of the three processes investigated are shown in Figure 1.

Table 1. Process parameters for Hammering Turning, vibration-assisted turning, and turning.

Parameter	Value
Cutting speed v_c and frequency of oscillation $f_{c,o}$	0.5 m/min (100 Hz) 1 m/min (200 Hz) 2 m/min (400 Hz)
Feed rate f_c	0.025; 0.05; 0.075; 0.1 mm/rev
Cutting depth a_p	0.1 mm
Hammer stroke a_H	10; 20; 30 µm
Tool ISO geometry	CCMW 120404
Rake angle γ / Clearance angle α	0° / 7°

2.2. Experimental materials

In this study, the quenched and tempered steel AISI 4140 (42CrMo4, material number 1.7225) was used. The

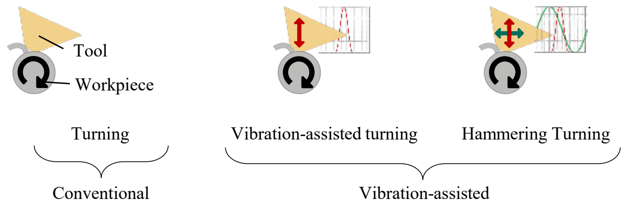

Figure 1: Kinematics of tool movement for turning (left), vibration-assisted turning (middle) and Hammering Turning (right)

mechanical properties of the material were determined by tensile tests and Vickers hardness measurements; the results are listed in Table 2. Samples with a diameter of 10 mm were used for the experimental tests. For the highly dynamic tool system, lightweight cutting inserts made of a titanium-containing cermet material were used, weighing only 3.66 g. The uncoated cutting inserts with ISO geometry CCMW120404 hade a corner radius of $r_\varepsilon = 0.4$ mm. This small radius allows local plastic deformation even at reduced process forces. The cutting edge radius was prepared by brushing using a silicon carbide nylon round brush. In this way, the cutting inserts were conditioned with a form factor of $K \leqslant 1$ and mean cutting edge rounding of $\overline{S} = 51.6 \pm 6.2$ µm. The cutting edge parameters were characterized and determined according to the method described by Denkena & Reichstein et al. [8].

Table 2. Material characteristics of AISI 4140/42CrMo4

Material properties	Value
Yield strength $R_{p0.2}$	1006.4 ± 2.4 MPa
Ultimate tensile strength R_m	1067.7± 2.1 MPa
Elongation at UTS A_g	5.76 ± 0.25%
Elongation to fracture A	14.60 ± 1.07%
Vickers hardness HV	383.6 ± 27.6 HV0.01

2.3. Radiographic residual stress measurement

The X-ray angle-dispersive residual stress measurement was carried out using an Xstress DR45 X-ray diffractometer from Stresstech GmbH and the Xstress Studio 1.4.0 evaluation software. The residual stresses were measured both in the feed direction (σ_{22}) and in the cutting direction (σ_{11}). Since measuring on curved surfaces can lead to an underestimation of the stress values, it must be ensured in accordance with DIN EN 15305 that the irradiated area is less than 0.4 times the radius of curvature. For the samples examined, this results in a maximum collimator size of 2 mm. However, to increase measurement reliability, a collimator diameter of 1 mm was selected in conjunction with an exposure time of 3 s. Further parameters of the X-ray tube are listed in Table 3. The goniometer arrangement of the diffractometer used corresponds to the modified χ method. The evaluation was performed using the $\sin^2\psi$ method, assuming a stress of $\sigma_{33} = 0$ MPa. To determine the residual stress depth profiles, the material must be removed layer by layer. Since mechanical or spark erosion methods can affect the stress state, an electrochemical method was used. The MoviPol-5 electrolytic polishing and etching device from Struers S.A.S. was used for this purpose. In the area close to the surface up to a depth of 100 µm, where high stress gradients are to be expected, a measurement interval of 10–20 µm was selected. In deeper areas, removal was carried out in steps of 30–50 µm. A voltage of 40 V was applied with exposure times of 20 s and 40 s, respectively. Material removal was recorded using a digital dial gauge (type ID-C, Mitutoyo) with a resolution of 0.5 µm.

Table 3. Parameters of X-ray residual stress measurement

Parameter	Value
Exposure time	3 s
Collimator size	1.0 mm
X-ray tube	Chrom
Material	Fe Ferritic {211} 156.4°
Calibration uncertainty	± 8 MPa
Transverse contraction factor	0.3
Modulus of elasticity	211,000 MPa
Rotation angle (φ)	2 (0° and 90°)
Tilt angle (ψ)	11 (-45° to 45°)
Acceleration voltage	30 kV
Current	9 mA

3. Results

The results of the surface residual stress components depending on the cutting speed v_c = 0.5–2 m/min are shown in Figure 2. For both vibration-assisted processes, pronounced compressive residual stresses occur in the stress components σ_{11} and σ_{22}. Conventional turning also generates compressive residual stresses, but to a significantly lower extent. The σ_{11} compressive residual stresses (cutting direction) for Hammering Turning increase slight with increasing cutting speed. For vibration-assisted turning, these are decreasing. It is noticeable that the values for Hammering Turning and vibration-assisted turning converge at higher cutting speeds, with vibration-assisted turning always exhibiting higher compressive residual stresses. In contrast, the compressive residual stresses in conventional turning decrease with the cutting speed. The σ_{22} compressive residual stresses (feed direction) decrease with the cutting speed for all three processes, most noticeably in Hammering Turning and turning. Here, the highest compressive residual stresses are achieved at low cutting speeds (v_c = 0.5 m/min). The measurements of the shear stress τ_{12} yield in much higher values. The lowest values were measured for the vibration-assisted processes at v_c = 2 m/min; at lower cutting speeds, they decrease. The opposite applies to conventional turning. Since the σ_{22} normal residual stresses in particular are strongly influenced by the cutting speed in Hammering Turning, this should be kept as low as possible in order to achieve high compressive residual stresses in the cutting direction.

The influence of the feed rate f_c was investigated in four stages between f_c = 0.025-0.1 mm/rev. The results of the stress measurements are shown in Figure 3 and reveal a behavior that is in contrast to the influence of the cutting speed. The σ_{11} compressive residual stress (cutting direction) decreases with increasing feed rate in all processes, but is lowest in vibration-assisted turning. The σ_{22} compressive residual stress increases slightly with higher feed rates. A greater distance between the tool paths thus leads to higher compressive stresses. This effect is most pronounced in conventional turning, while it is less dominant in Hammering Turning and vibration-assisted turning. The shear stresses τ_{12} are significantly more sensitive to the feed rate. In vibration-assisted processes, they decrease sharply with increasing feed rate and reach values similar to

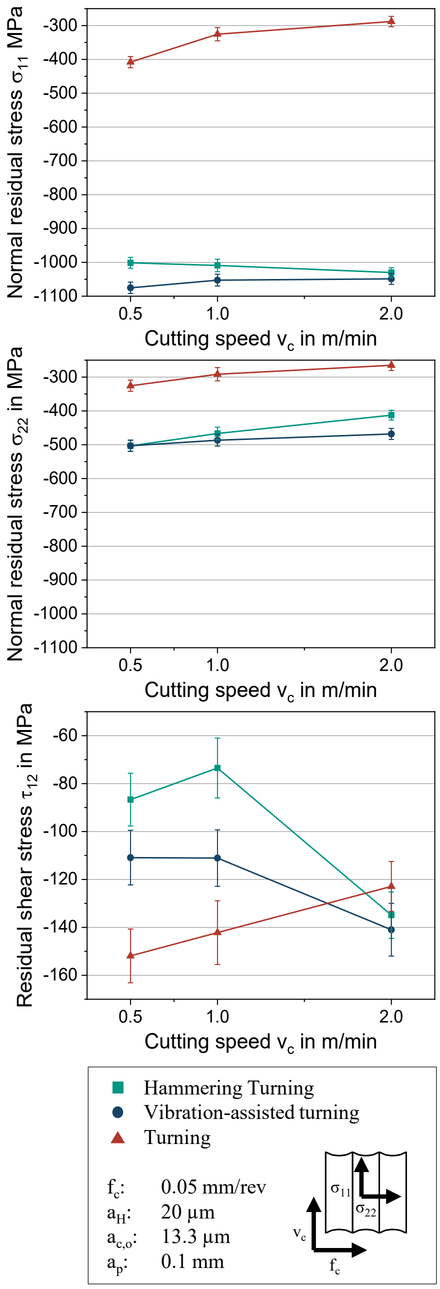

Figure 2: Influence of cutting speed v_c on the residual stresses σ_{11}, σ_{22}, and τ_{12} at the surface

those in turning for $f_c = 0.1$ mm/rev. A higher feed rate therefore results in greater absolute shear stress on the surface. Small feed values should therefore be selected to generate high compressive residual stresses with low shear stresses.

The hammer stroke a_H represents the process parameter that differs between Hammering Turning and vibration-assisted turning from conventional turning. The resulting residual stresses for hammer strokes between a_H = 10–30 µm are shown in Figure 4. For the σ_{11} component in the cutting direction, the higher compressive residual stresses are evident in vibration-assisted turning, regardless of the stroke size – a result that has already been observed in the investigation of other process parameters. The maximum compressive residual stress occurs for both processes at a hammer stroke of a_H = 20 µm. A comparable profile can be seen for the σ_{22}-component. This leads to the conclusion that a small hammer stroke does not cause sufficient plastic deformation, while an excessively large hammer stroke leads to a reduction in compressive residual stresses due to increased material flow. At the same time, the lowest shear stresses τ_{12} occur in this area. The optimum hammer stroke for hammering and vibration-assisted turning is therefore a_H = 20 µm.

3.1. Residual stress depth profiles

Figure 5 shows the X-ray-determined residual stress depth profiles of the samples for the σ_{11} and σ_{22} components from Hammering Turning, vibration-assisted turning, and conventional turning. The two vibration-assisted processes show a significant build-up of compressive residual stresses (σ_{22} < -450 MPa, σ_{11} < -1000 MPa). Conventional turning also produces significant compressive residual stresses on the surface due to the low cutting speed and large cutting edge rounding. However, these only reach a depth of about 50 µm and then taper off. For the σ_{22} stress component (feed direction) of vibration-assisted processes, the typical profile for mechanical surface treatments is obtained with a minimum below the surface. In both cases, this is at a depth of approximately 100 µm, while the compressive residual stresses extend into the surface layer to a depth of over 200 µm. The compressive residual stresses are slightly more pronounced in Hammering Turning than in vibration-assisted turning, with σ_{22} < -500 MPa. The σ_{11} component (cutting direction) shows a minimum and thus a maximum in compressive residual stress directly at the surface and extends into the surface layer to a similar depth as the σ_{22} component. Here, vibration-assisted turning exhibits slightly higher compressive residual stresses (σ_{11} < -1150 MPa) than Hammering Turning. Overall, vibration-assisted turning and Hammering Turning exhibit very similar residual stress depth profiles, both in terms of shape and magnitude. The evaluation of the τ_{12} residual shear stress component shows clear differences between Hammering Turning and vibration-assisted turning. Shear stresses of τ_{12} < -145 MPa were measured on the surface of the turned samples. A similar level is also found in vibration-assisted turning, but here the shear stress extends to over 200 µm into the surface layer. The stress profile shows a plateau near the

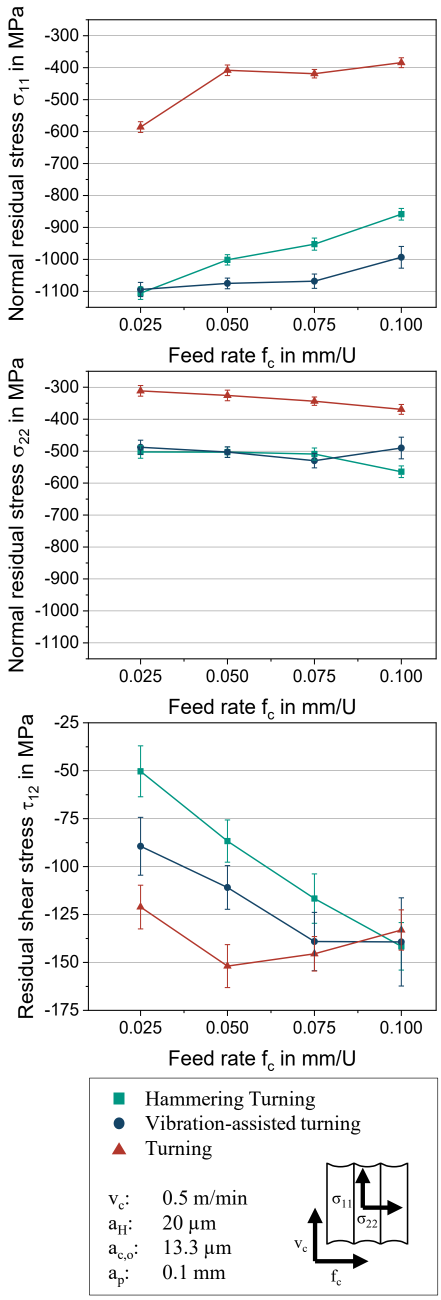

Figure 3: Influence of feed rate f_c on the residual stresses σ_{11}, σ_{22}, and τ_{12} at the surface

surface and continues to decrease towards the surface. This illustrates that the mechanical surface treatment in combination with the superimposed sliding movement causes strong shearing in the surface layer and that the machining character of the process is retained. In Hammering Turning, on the other hand, the shear stresses are significantly lower in terms of magnitude and reach a minimum of τ_{12} < −90 MPa at a depth of about 50 µm. The qualitative profile also differs: The shear stresses do not decrease towards the surface, as is the case in the other processes, but increase and only reach τ_{12} -50 MPa there. This indicates lower shear stress in the surface layer. In addition, the depth effect is lower than with vibration-assisted

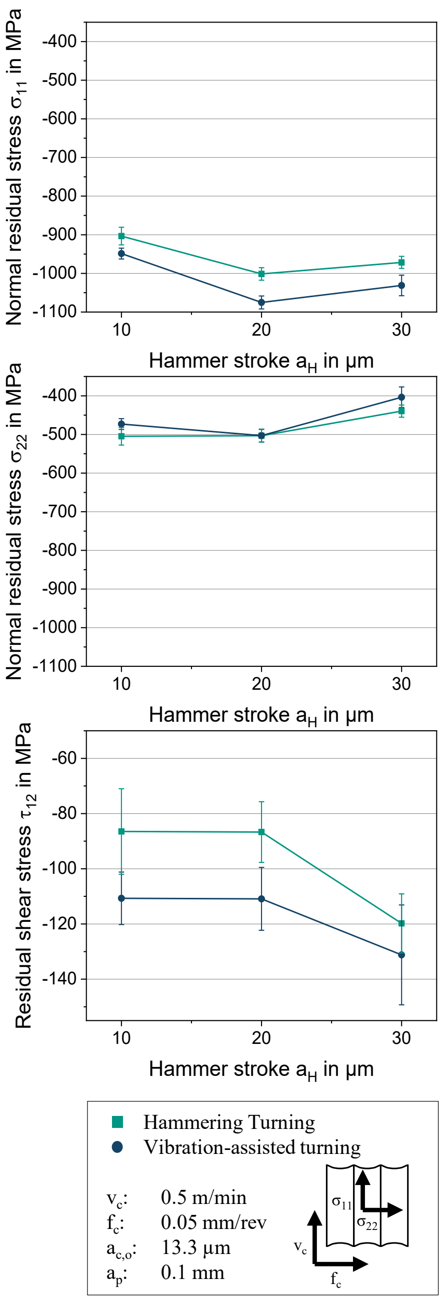

Figure 4: Influence of hammer stroke a_H on the residual stresses σ_{11}, σ_{22}, and τ_{12} at the surface

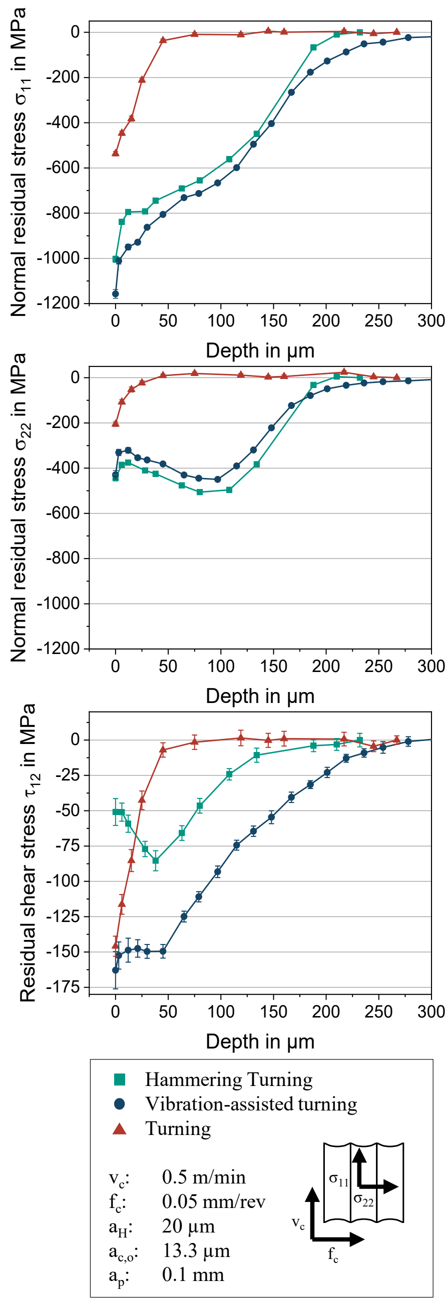

Figure 5: Residual stress depth profiles σ_{11}, σ_{22}, and τ_{12} resulting from Hammering Turning, vibration-assisted turning, and turning

turning and only extends to about 150 µm. The residual stress depth profiles show that the vibration-assisted processes achieve mechanical surface treatment to a depth of approx. 200 µm. This leads to a significant increase in compressive residual stresses with a profile typical for such processes.

4. Discussion

The process parameters influence the residual stress components. An increase in cutting speed leads to higher compressive residual stresses in the cutting direction in vibration-assisted processes, while they decrease in the feed direction. In conventional turning, on the other hand, the compressive residual stresses decrease in both directions. These differences can be explained by the higher deformation rate, which is increased by a factor of four. In the cutting direction, this results in a different process character compared to turning, while in the feed direction, a similar character remains. Higher feed rates lead to a reduction in compressive residual stresses in the cutting direction for all processes, while they increase in the feed direction. This illustrates that a minimum distance between the tool paths is required for the formation of high normal compressive residual stresses, so that a compromise must be found between cutting speed and feed rate. The highest shear residual stresses occur at high feed rates (f_c = 0.1 mm/rev), with values similar to those for conventional turning. In Hammering Turning, the material flow can reduce the shear stress on the surface, which results in low shear residual stresses. The hammer stroke a_H has the greatest influence on the residual stresses in the feed direction. As the stroke increases, the compressive residual stresses decrease there, while they increase slightly in the cutting direction and reach their maximum at $a_H = 20$ µm. This clearly shows that excessive plastic deformation reduces the formation of compressive residual stresses, but at the same time a minimum amount of plastic deformation is necessary to introduce them. The investigation of the influence of process parameters on residual stresses at the surface shows that high compressive residual stresses can be introduced into the surface layer by selecting the feed rate, cutting speed, and hammer stroke.

Compared to vibration-assisted machining of titanium alloys, higher compressive residual stresses can be achieved with quenched and tempered AISI 4140 steel. During experimental machining of Ti6Al4V, Maroju et al. achieved compressive residual stresses of only up to -338.4 MPa in the vertical direction [6]. Simulations of the same material by Kurniawan et al. yielded similarly high values, with compressive residual stresses calculated to reach up to 400 MPa in 2D VAM [5]. These differences can be attributed to the different materials and the titanium alloy's significantly lower Young's modulus. The measurements of depth profiles show only low tensile residual stresses, but higher compressive residual stresses near the surface. The measured σ_{11} profiles in the cutting direction show a maximum compressive residual stress directly at the surface, as is typical for near-surface stretching. The low cutting speed during conventional tuning results in low temperatures, which prevents thermally induced tensile residual stresses. In vibration-assisted processes, the additional plastic deformation causes increased stretching. In Hammering Turning, however, the unavoidable tangential sliding component means that a pure Hertzian pressure profile is not apparent. Instead, a saddle point appears below the surface, with compressive residual stresses that are slightly lower than in vibration-assisted turning. In the feed direction (σ_{22}-component), the minima for both Hammering Turning and vibration-assisted turning are below the surface, which corresponds to the typical profile of Hertzian pressure. The reason for this is the negligible sliding component in the feed direction, so that there is hardly any surface elongation. The residual stress profiles of both processes are nearly identical. Due to the plastic deformation resulting from the reduced cutting speed in Hammering Turning, the profile approaches the ideal Hertzian pressure more closely, with slightly higher compressive residual stresses than in vibration-assisted turning without cutting speed reduction. Overall, the residual stress profiles for both vibration-assisted processes show typical characteristics of mechanical surface treatment with compressive residual stresses reaching depths of over 200 µm [9]. The residual shear stresses illustrate that vibration-assisted turning exhibits similar shear behavior to turning, with the minimum occurring at the surface. In contrast, a significant reduction in shear stresses at the surface was observed for Hammering Turning.

5. Summary

The study examined the influence of process parameters on residual stresses in vibration-assisted processes such as Hammering Turning, vibration-assisted turning, and conventional turning as a reference. The cutting speed primarily influences the compressive residual stresses in the cutting direction: vibration-assisted processes produce higher compressive residual stresses, which increase with increasing cutting speed, while the opposite trend can be observed in conventional turning. Feed rate has the opposite effect: higher values lead to lower compressive stresses in the cutting direction, but to higher compressive residual stresses in the feed direction. An optimal stroke of $a_H = 20$ µm was determined, as small strokes do not cause sufficient plastic deformation and large strokes reduce compressive stresses due to excessive material flow. The residual stress depth profiles confirm that both vibration-assisted processes generate characteristic compressive stresses that are typical for mechanical surface treatments and extend to a depth of more than 200 µm, while conventional turning is limited to about 50 µm. The process can cause compressive stresses down to $\sigma_{11} < -1000$ MPa in the cutting direction. Compared to vibration-assisted turning, Hammering Turning results in slightly higher compressive stresses in the feed direction, but lower stresses in the cutting direction

Overall, the results show that the vibration-assisted processes of Hammering Turning and vibration-assisted turning can introduce high compressive residual stress states into components.

Acknowledgements

The authors thank the German Research Foundation for funding this study as part of the research project ZA 785/4-2.

References

[1] Brehl, D.E., Dow, T.A., 2008. Review of vibration-assisted machining 32, p. 153.
[2] Skelton, R.C., 1968. Turning with an oscillating tool 8, p. 239.
[3] Greco, A., Raphaelson, S., Ehmann, K., Wang, Q.J. et al., 2009. Surface Texturing of Tribological Interfaces Using the Vibromechanical Texturing Method 131.
[4] Huang, X.-D., Zhang, X.-M., Leopold, J., Ding, H., 2018. Analytical Model for Prediction of Residual Stress in Dynamic Orthogonal Cutting Process 140.
[5] Kurniawan, R., Ahmed, F., Ali, S., Park, G.C. et al., 2021. Analytical, FEA, and experimental research of 2D-Vibration Assisted Cutting (2D-VAC) in titanium alloy Ti6Al4V 117, p. 1739.
[6] Maroju, N.K., Pasam, V.K., 2019. FE Modeling and Experimental Analysis of Residual Stresses in Vibration Assisted Turning of Ti6Al4V 20, p. 417.
[7] Schwalm, J., Mann, F., Gerstenmeyer, M., Zanger, F., 2022. Main time-parallel mechanical surface treatment and surface texturing during machining 108, p. 240.
[8] Denkena, B., Reichstein, M., Brodehl, J. & Leon-Garcia, L. Surface Preparation, Coating and Wear Performance of Geometrically Defined Cutting Edges 2005.
[9] Schütz, W., 1993. Mechanische Oberflächenbehandlung – Festwalzen, Kugelstrahlen, Sonderverfahren.) DGM Informationsgesellschaft 24, p. 249.